Saturation in a Ni-like Pd soft-x-ray laser at 14.7 nm

R. Tommasini,* F. Löwenthal, and J. E. Balmer
Institute of Applied Physics, University of Bern, Sidlerstrasse 5, CH-3012 Bern, Switzerland
(Received 22 June 1998; revised manuscript received 14 September 1998)

Here we report on what is to our knowledge, the first achievement of saturated output in a collisionally pumped, Ni-like Pd soft-x-ray laser at 14.7 nm ($J=0$-1 line). Using a single prepulse scheme and a 100-ps pulse duration we were able to observe the onset of saturated output and to measure a gain-length product of 15.8 (gain=8.3 cm^{-1}) on flat slab targets. A systematic investigation and discussion on beam divergence, deflection angle, and space-resolved measurements is also presented. All these aspects lead to the evidence of the onset of saturation. The measured drive-irradiance threshold for the x-ray laser emission was only 6.6 TW/cm^2 ($\approx$165 GW) while the maximum used drive irradiance was only 12 TW/cm^2 ($\approx$300 GW). These values correspond, respectively, to a pump energy of 16.5 J and 30 J in 100 ps and demonstrate the realization of a real table-top soft-x-ray laser. A key role in the achievement of these results was played by the reduction in the roughness of the target surface, which greatly improves the performances of the Pd x-ray laser.
[S1050-2947(99)00502-8]

PACS number(s): 42.55.Vc, 32.30.Rj, 42.60.By

I. INTRODUCTION

The possibility to produce short-wavelength lasers is of fundamental importance in many fields such as holography, biological microscopy, interferometry, radiography and x-ray lithography. As an example, progress in chip structure miniaturization depends on shorter wavelengths for wafer steppers. Deep UV steppers, coming into the chip manufacturing process on a large scale worldwide, use excimer lasers at 248 nm. Hence, decisive progress will come from using soft-x-ray laser sources and the wavelengths in the range of 15–12 nm seem to be the most promising in the near future [1].

Saturated operation of soft-x-ray lasers is important because it assures the maximum stimulated emission power extraction from a given volume of excited plasma. Saturation has been previously achieved in Ne-like schemes, see, for example, [2–6], and recently also by our group [7]. However, because of the intrinsic rapid increase in the pump power required to achieve saturated operation, Ne-like schemes are difficult to scale to wavelengths shorter than 20 nm. Because of this it is natural to exploit the more favorable scaling of required pump power of the Ni-like schemes, which, on the other hand, have more difficulties in providing saturated output.

In this context many groups of researchers have reported significant progress and multipulse irradiation has been successfully used to produce x-ray laser action in a number of elements [8–10] at a considerably lower irradiance than in single pulse irradiation schemes [11]. In a series of experiments on Ni-like ions, Daido *et al.* [10,12] reported soft-x-ray lasing in Ni-like Ag, Te, La, Ce, Pr, and Nd, covering the spectral range 14.3–7.9 nm, using a three-prepulses configuration. In particular, a gain of 2 cm^{-1} and a gain-length product of 5 were found for Ag using an average irradiance of 70 TW/cm^2. In these works it is outlined how, despite the gain coefficients of the Ni-like lasers being almost the same as those of Ne-like lasers, the output energy of the Ni-like lasers is much smaller, probably because of the smaller size of the gain region. With a different scheme, irradiance up to 10 TW/cm^2 and a low-energy prepulse train (2%) preceding the main pulse, Ros *et al.* [13] have been able to measure lines from 2-cm and 1-cm target lengths indicating a small gain (0.75 ± 0.6 cm^{-1}) for tin, while for silver they reported the evidence of a 2 times weaker line than for tin. More recently, Li *et al.* [14,15] demonstrated lasing in the 12-nm, $J=0$-1 $4d$-$4p$ transition on Ni-like Sn with a gain-length product of about 4.8 using curved targets, a single 7.5% prepulse, and a total energy of 500 J in 450 ps. Lasing in the $4d$-$4p$ $J=0$-1 line of Ni-like Pd has recently been obtained by Dunn *et al.* [16]. Using the transient collisional excitation scheme and irradiation of a slab target by two laser pulses (a formation beam with 5 J energy of 800-ps duration and a pump beam of 5 J energy in 1.1 ps) with an 8-mm line focus, they reported a gain-length product of 12.5 at 14.7 nm. Drive irradiance was about 60 TW/cm^2, with no indication of saturation in the x-ray laser output.

Only recently a high gain-length product (at around 15) and hence evidence of saturation, has been reported for Ni-like elements. Zhang *et al.* [17] obtained the first evidence of saturation in a Ni-like x-ray laser, specifically a Ni-like Ag x-ray laser at 14 nm from a double flat target irradiated with about 20 TW/cm^2, corresponding to an energy of about 75 J. The gain-length product measurement gave a value of 16 and a gain coefficient of 7.2 ± 0.4 cm^{-1}. The laser emission divergence was 1.7 mrad, with a source size of (43×57) μm^2. Using a similar set up, Zhang *et al.* [18] also showed saturation in a Ni-like samarium x-ray laser at 7 nm.

Here we report achievement of saturated output in a collisionally pumped, nickel-like Pd x-ray laser at 14.7 nm ($J=0$-1). The pumping scheme used is a single 8% prepulse 1 ns before the 100-ps main pulse. A detailed study of the surface roughness of the target led to the usage of diamond machined, 23-mm-long, flat Pd slab targets. This made it possible to reach the saturated regime, decreasing the threshold for laser action from 8.4 to 6.6 TW/cm^2 with respect to a

*Electronic address: tommasini@iap.unibe.ch

standard machined target, with a corresponding factor-of-4 improvement in slope efficiency. The measured gain coefficient is 8.3 cm^{-1} with a gain-length product of 15.8 (19-mm target length). The maximum drive irradiance was only 12 TW/cm^2, corresponding to an energy of 30 J, by far the lowest ever used in Ni-like schemes showing saturation.

II. EXPERIMENTAL SETUP

The experiments were performed using the 1054-nm Nd:glass laser at the Institute for Applied Physics of the University of Bern. The system [7,19] is capable of delivering up to 300 GW ($=12$ TW/cm^2 for a 2.5×10^{-2}-cm^2 line focus) at a pulse duration of 100 ps full width at half maximum (FWHM). A line focus of 2.5 cm length and approximately 100 μm width is produced using a combination of an aplanatic doublet and a cylindrical lens resulting in an f number of 6. A defined prepulse at a variable delay was obtained by inserting a beam splitter into an optical delay line after the last (90 mm diameter) amplifier stage. The beam splitter has a reflectivity of 8% at 1.054 μm and generates a prepulse with variable time delay, varying the distance of the beam splitter from the main mirror. The best results were obtained with a 1-ns delay. The spatial coincidence of the prepulse line focus and the main pulse line focus was adjusted to an accuracy of ±8 μm at the target surface. Varying the gain in the preamplifier rods varied the energy of the main pulse between 5 and 12 TW/cm^2, for threshold and slope efficiency measurements. The targets used were flat slabs of the pure material. The best results were obtained with diamond-machined targets. All the targets had a length of up to 2.3 cm and the line focus was aligned in order to slightly overfill the target on the spectrometer side. The main diagnostics were an on-axis, time-integrating spectrometer that could be configured in either an angle- or space-resolving arrangement. The spectrometer consists of a 1200 grooves/mm, aberration-corrected, concave reflection Hitachi grating (radius of curvature: 5649 mm), working at a grazing-incidence angle of 3°. The grating disperses the incident radiation perpendicular to the direction of the spatial/angular resolution on a 40-mm-diameter P20 phosphor screen, which is imaged to a cooled charge-coupled device camera with a pixel size of 25 μm$\times$25 μm. The one-dimensional spatial resolution of about 15 μm perpendicular to the target surface was realized by using a spherical gold mirror with a radius of curvature of 2 m adjusted at a grazing-incidence angle of 5.5°, to form an image of the plasma column on the phosphor screen with a magnification of $3\times$. The diameter of the gold mirror was 30 mm and the acceptance angle of the spectrometer was 22 mrad. The wavelength coverage of the spectrometer was 12 nm with a spectral resolution of 0.2 nm. For the angle-resolved measurements the imaging gold mirror was removed and a 50 μm aluminum wire was positioned in front of the spectrometer to serve as an angular reference. The 1054-nm pump pulse was constantly monitored using a calibrated optical streak camera, resulting in a pulse width of 100 ± 10 ps.

III. RESULTS AND DISCUSSION

Figure 1 shows a typical spectrum emitted by Ni-like Pd, using a flat diamond-machined target of 2.3 cm length. The

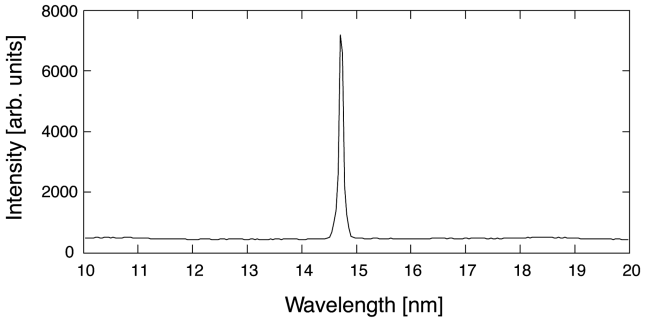

FIG. 1. Soft x-ray laser spectrum from flat Pd target. The $4d\,^1S_0$-$4p\,^1P_1$ line is clearly predominant on the background spectrum.

$4d\,^1S_0$-$4p\,^1P_1$ transition ($J=0$-1 B line in the Scofield-MacGowan notation [20]) is clearly predominant on the background spectrum.

During the experiment great attention was paid to the roughness of the target surface. It turned out that even very small irregularities of the surface extended to the formed plasma thus affecting beam propagation and hence effective gain. A substantial improvement was achieved by decreasing the typical surface roughness along the line focus direction by an order of magnitude, using diamond-machined Pd targets, passing from 0.7 to 0.07 μm (as standard deviation from perfect flatness). Figure 2 shows a comparison between the surface profile along the direction of the line focus for a standard-machined target (dotted line) and a diamond-machined target (solid line). The target surface optimization produced three main results: (i) a substantial decrement of the $J=0$-1 Ni-like Pd laser threshold, from 8.4 TW/cm^2 to 6.6 TW/cm^2, i.e., from 210 GW to 165 GW, (ii) a noticeable increment of a factor of 4, in the slope efficiency, and (iii) a factor-of-8 increment in the emitted laser intensity at a pump irradiance of 10 TW/cm^2. These results are evident from Fig. 3, where the x-ray laser intensity output vs drive irradiance measurements from a diamond-machined target (squares) and a standard machined target (crosses) are reported in order to have a comparison of the respective thresholds and slope efficiencies. Similar results were obtained in an analogous experiment using Ag and demonstrate the decisive role of the target-surface quality.

A series of measurements for the optimization of the target curvature and the main pulse-prepulse time delay were performed, in another experiment involving also Ag, Sn, and

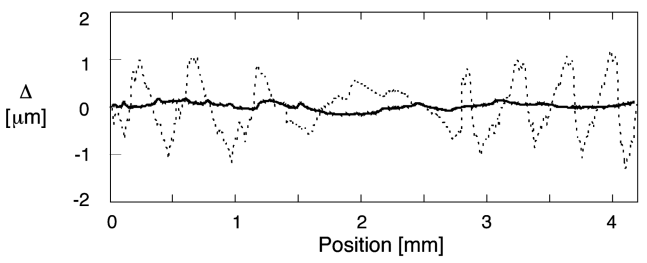

FIG. 2. Profiles of the target surface along the direction of the line focus (fresh target): the dotted line represents data for a standard-machined target while the solid line represents data for a diamond-machined target.

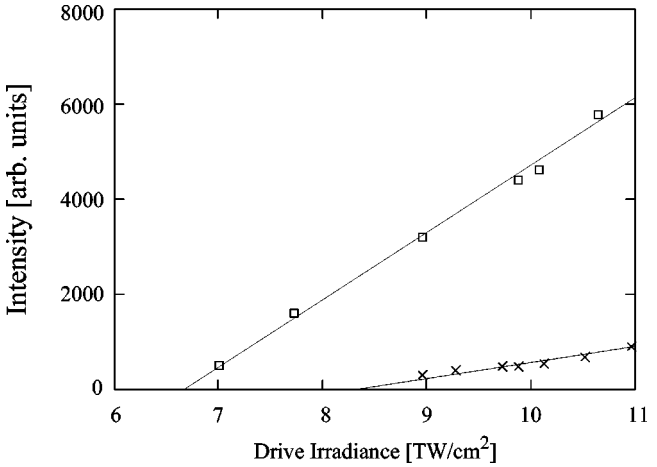

FIG. 3. X-ray laser peak intensity vs drive irradiance. Squares represent data from a diamond-machined target, crosses represent data from a standard machined target. Threshold shows a decrement from 8.4 TW/cm^2 to 6.6 TW/cm^2. Slope efficiencies are in the ratio of 4.

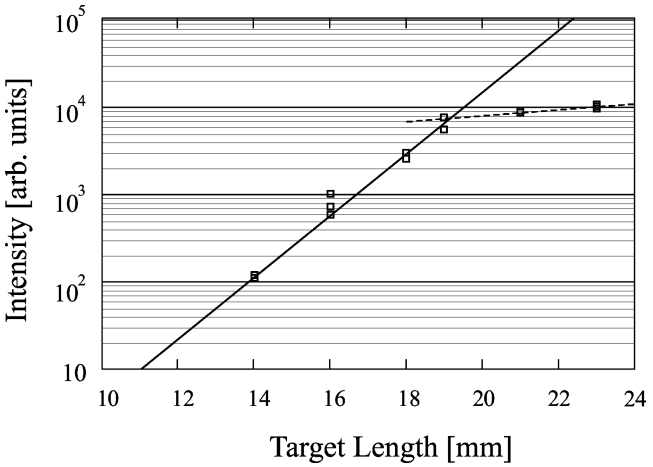

FIG. 4. Peak intensity vs target length for Ni-like Pd at 14.7 nm. The solid line represents a fit using the Linford formula. Resulting gain coefficient is 8.3. Saturation arises at a gain-length product of 15.8. The dashed line represents a fit using a linear curve, hence demonstrating departure from Linford-like behavior, i.e., saturation.

In. Selected curvature radii were 1.5, 3, and 6 m and ∞ (flat). The prepulse time delays were 0.5, 1.0, 1.5, 2.0, and 2.5 ns, while the level was maintained at 8% of the main pulse. All these elements show a pronounced peak in the emitted power for flat targets and for a 1.0-ns prepulse delay. In order to make the study on the target curvature more complete some measurements of the far-field deflection angle of the x-ray laser beam φ_∞ were performed using flat 23-mm-long targets, to estimate the optimum curvature radius. Given a target of length L, the optimum curvature radius R is given by $R \cong L/\varphi_\infty$. Since it results in a value for the measured far-field deflection angle of $\varphi_\infty = (2.2 \pm 0.3)$ mrad, the optimum target curvature radius thus obtained is about 11 m, which is indeed near to flat. The result of a pronounced peak in the x-ray laser output in correspondence of a specific target curvature (even if near to flat) and a specific pulse delay time is in agreement, in the sense that for Ni-like ions both prepulse and target curvature need to be optimized, with the work of Li *et al.* [15] in which it is demonstrated that for Ni-like ion lasers, the target curvature is equally important as the prepulse. We also tested some double prepulse schemes, which showed no clear advantage over the single prepulse scheme.

As a consequence of these results the setup of choice for the gain-length product measurements was a flat slab Pd target, diamond-machined and an 8% prepulse 1.0 ns before the main pulse.

In Fig. 4 we show the results of the gain-length measurements together with a curve representing the best fit to the formula of Linford *et al.* [21]. The measured gain is 8.3 cm^{-1} and the corresponding gain-length product is 15.8 for a target length of 19 mm. The efficiency parameter of producing gain [22] is calculated at 10 TW/cm^2 (250 GW) giving the high value of $(GL)_{sat}/P = 63$ TW^{-1}. The departure from the fit of Linford *et al.* at approximately 19 mm of target length, the linear behavior of the emitted intensity for longer target lengths and the high gain-length product are all evidences of the onset of saturation.

Figure 5 gives the dependence of the angular divergence on the target length. The results are qualitatively analogous to what was reported by Chilla and Rocca [23] using Ne-like argon in the capillary discharge configuration. The beam divergence decreases with increasing target length, reaching a minimum almost 1.3 mm before the value corresponding to the saturation length and then shows a nearly constant behavior for longer target lengths. This behavior is consistent with the onset of saturated gain. Rebroadening at longer target lengths is not evident.

From the far-field beam divergence (2.0 ± 0.2) mrad, for target lengths larger than 18 mm (see Fig. 5), it is possible to measure the transverse coherence length l_c at the end of the gain medium [24–26]. The result is $l_c = (2.4 \pm 0.2)$ μm. As a comparison, Daido *et al.* [27] reported a transverse coherence length of about 3.7 μm for the 19.6-nm line of the Ne-like germanium.

The value of the far-field beam divergence suggests a diameter for the gain region, and for a 19-mm-long target, of about 38 μm. This has been confirmed by some space resolved measurements. Figure 6 shows indeed a scan along the spatial coordinate for the near field intensity distribution

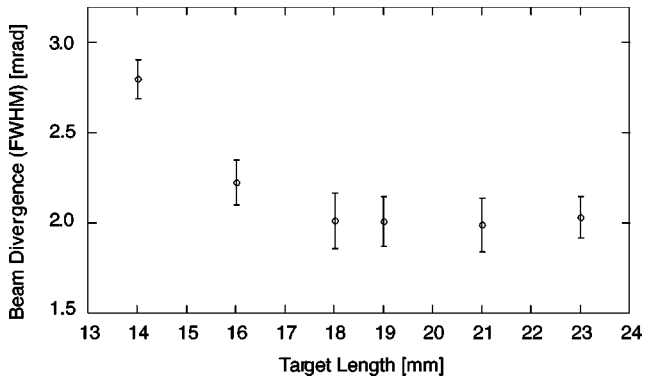

FIG. 5. Beam divergence of x-ray laser emission from flat Pd target vs target length: the divergence decreases reaching its minimum approximately 1.3 mm before the value corresponding to the saturation length and then shows a nearly constant behavior for longer target lengths, consistent with the onset of saturated gain. Rebroadening at longer lengths is not evident.

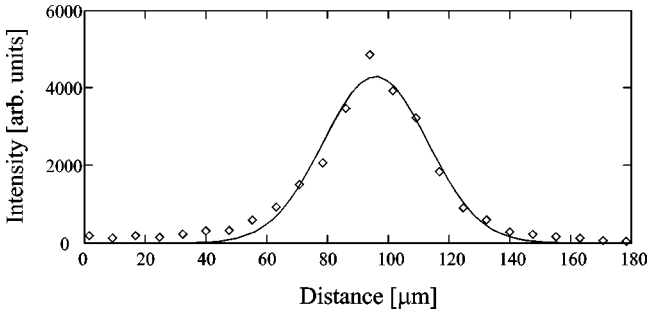

FIG. 6. Typical scan along the spatial coordinate for the near field intensity distribution of the 14.7-nm emission line for a 19-mm-long Pd target irradiated at 10 TW/cm^2, together with a best fit to a Gaussian distribution. It can be inferred that the lasing line is emitted by an approximately 40-μm-wide gain region (FWHM).

of the 14.7-nm emission line for a 19-mm-long Pd target irradiated at 10 TW/cm^2, together with a best fit to a Gaussian distribution, in order to better estimate the width of the line. It can be inferred that the lasing line is indeed emitted by an approximately 40-μm-wide gain region (FWHM). Notice that this value is about a factor of 16 larger than the transverse coherence length and is very near to what was reported by Zhang *et al.* [17] for Ag.

As a comparison with the experimental results we report the formula for maximum gain-length product at the onset of saturation. The relation valid for the spectrally integrated line intensity is [21,28] $(e^{GL}/\sqrt{GL})_{sat}=4\pi\eta(\tau_{21}/\tau_2)\Delta\Omega^{-1}$, where $\eta\equiv 1-(g_2N_1/g_1N_2)$ is the inversion fraction, τ_{21} and τ_2 are, respectively, the radiative lifetime and the total lifetime of the upper laser level, and $\Delta\Omega$ is the solid angle for the amplified spontaneous emission (ASE) output. Assuming, as is common practice, the constant $C\equiv\eta\tau_{21}/\tau_2\simeq 1$ and using a radius of 20 μm for the gain region or, equivalently, a value of 2 mrad for the far-field beam divergence, the above relation gives a gain coefficient of 8.5 ± 0.3 cm^{-1} and a gain-length product of 16.2 ± 0.6, values that are consistent with the experimental measurements here reported. We note that this result is mainly qualitative. Actually the ratio of the decay times τ_{21}/τ_2 can be very large, even two orders of magnitude [2], as a consequence of the important effect of collisional depopulation of the upper laser level. The error in approximating C to 1 is, however, much less, because η is typically less than 1, thus somewhat balancing the τ_{21}/τ_2 factor. In any case, when the approximation is not valid, the predicted values have to be increased, as a first-order correction factor, by the quantity $\ln(C)$; hence, $(GL)_{sat}$ has to be replaced by $(GL)_{sat}+\ln(C)$. Notice that the second-order analysis would give an extra-additive correction factor of $2^{-1}\ln[1+\ln(C)/GL]$, which is negligible, for typical values of C and GL, with respect to $\ln(C)$.

Finally we want to use the measurement of the far-field deflection angle φ_∞ to estimate the maximum electron density traversed by the emerging x-ray beam. Using the relation [23,29] $N_0=2N_c[1-\exp(-\varphi_\infty^2/2)]$, where the critical electron density is given by [30] $N_c=1.1\times 10^{21}\lambda^{-2}$ [cm^{-3}] (λ in μm) and the measured value for φ_∞ of (2.2 ± 0.3) mrad, in the case of our experiments on Pd, the relation gives $N_{0,\mathrm{exp}}=(2.4\pm 0.8)\times 10^{19}$ cm^{-3}. Hence, following Elton [31], we can assume an optimum electron density of $N_{opt}=N_0/2=(1.2\pm 0.4)\times 10^{19}$ cm^{-3}.

IV. CONCLUSIONS

Saturation in a collisionally excited Ni-like Pd x-ray laser at 14.7 nm ($4d\,^1S_0$-$4p\,^1P_1$ line) has been demonstrated through a systematic investigation on gain-length measurements and spatial and angular beam characterization. Reducing the target surface roughness, which greatly improves the laser performances, and using an optimized target curvature and a single prepulse scheme with 100-ps pulse duration, we were able to measure a gain coefficient $g=8.3$ cm^{-1} and a gain-length product of 15.8. Investigation on the far-field deflection angle and space-resolved measurements have also been presented, leading to the experimental maximum electron density measurement and to the comparison with the formula of Linford *et al.* for the maximum gain-length product. The pump energy was varied in the range between 16 and 30 J, by far the lowest ever used, up to date, in soft-x-ray laser from Ni-like ions showing saturation.

ACKNOWLEDGMENTS

The authors would like to thank H.P. Weber for continuous encouragement and B. Locher and W. Lüscher for their technical assistance with the target preparation. This work was supported by the Swiss National Science Foundation.

[1] H. Hinkelmann, in *Focus on Detectors and Cameras*, special issue of EuroPhotonics, December, 32 (1998).
[2] A. Carillon *et al.*, Phys. Rev. Lett. **68**, 2917 (1992).
[3] J. A. Koch *et al.*, Phys. Rev. Lett. **68**, 3291 (1992).
[4] L. B. Da Silva *et al.*, Opt. Lett. **18**, 1174 (1993).
[5] J. J. Rocca *et al.*, Phys. Rev. Lett. **77**, 1476 (1996).
[6] J. Zhang *et al.*, Phys. Rev. A **54**, R4653 (1996).
[7] F. Loewenthal, R. Tommasini, and J. E. Balmer, Opt. Commun. **154**, 325 (1998).
[8] J. Nilsen and J. C. Moreno, Opt. Lett. **20**, 1386 (1995).
[9] H. Daido *et al.*, Phys. Rev. Lett. **75**, 1074 (1995).
[10] H. Daido *et al.*, Opt. Lett. **21**, 958 (1996).
[11] B. J. MacGowan *et al.*, Phys. Fluids B **4**, 2326 (1992).
[12] H. Daido, in *X-ray Lasers*, edited by S. Svanberg and C-G. Wahlstroem, IOP Conf. Proc. No. 151 (Institute of Physics, London, 1996), p. 40.
[13] D. Ros, in *X-ray Lasers* (Ref. [12]), p. 50.
[14] Y. Li *et al.*, Phys. Rev. A **53**, R652 (1996).
[15] Y. Li *et al.*, Phys. Plasmas **4**, 479 (1997).
[16] J. Dunn *et al.*, Phys. Rev. Lett. **80**, 2825 (1998).
[17] J. Zhang *et al.*, Phys. Rev. Lett. **78**, 3856 (1997).
[18] J. Zhang *et al.*, Science **276**, 1097 (1997).
[19] A. R. Praeg *et al.*, Appl. Phys. B: Lasers Opt. **B66**, 561 (1998).
[20] J. H. Scofield and B. J. MacGowan, Phys. Scr. **46**, 361 (1992).

[21] G. J. Linford *et al.*, Appl. Opt. **13**, 379 (1974).
[22] M. H. Key, J. Mod. Opt. **35**, 575 (1988).
[23] J. L. A. Chilla and J. J. Rocca, J. Opt. Soc. Am. B **13**, 2841 (1996).
[24] J. Perina, *Coherence of Light* (Van Nostrand/Reinhold, London, 1971).
[25] M. Born and E. Wolf, *Principles of Optics* (Pergamon Press, New York, 1975).
[26] E. Collett and E. Wolf, Opt. Commun. **32**, 27 (1980).
[27] H. Daido *et al.*, Opt. Lett. **20**, 61 (1995).
[28] R. A. London, Phys. Fluids **31**, 184 (1988).
[29] E. E. Fill, J. Opt. Soc. Am. B **14**, 1505 (1997).
[30] L. B. Da Silva *et al.*, Phys. Rev. Lett. **74**, 3991 (1995).
[31] R. C. Elton, *X-RAY Lasers* (Academic Press, New York, 1990).